



HAL
open science

Conservative vs. non-conservative diusion towards a target in a networked environment

Ernesto Estrada

► **To cite this version:**

Ernesto Estrada. Conservative vs. non-conservative diusion towards a target in a networked environment. The Target Problem, In press. hal-04229218v4

HAL Id: hal-04229218

<https://hal.science/hal-04229218v4>

Submitted on 25 Jan 2024

HAL is a multi-disciplinary open access archive for the deposit and dissemination of scientific research documents, whether they are published or not. The documents may come from teaching and research institutions in France or abroad, or from public or private research centers.

L'archive ouverte pluridisciplinaire **HAL**, est destinée au dépôt et à la diffusion de documents scientifiques de niveau recherche, publiés ou non, émanant des établissements d'enseignement et de recherche français ou étrangers, des laboratoires publics ou privés.

Conservative vs. non-conservative diffusion towards a target in a networked environment

Ernesto Estrada

Abstract The networked nature of complex systems determines the way in which 'information' navigates the system from a source to a target. This navigation is governed by the lack of central controllers and the fact that every individual entity ignores the global structure of the system. Consequently, targeted shortest-path searches are almost automatically excluded in these systems, leaving the more blind diffusive processes as the main mechanism for navigating complex networks. Here we show that non-conservative diffusion has some advantages over the 'classical' (conservative) diffusion for searching a target in a network. The non-conservative nature of the diffusion process is given by the possibility that the network 'communicates' with the environment in which it is embedded. We use analytical and computational methods to show that non-conservative diffusion uses trajectories which are more prone to find a target than the conservative one. We illustrate the existence of this mechanisms in systems as varied as traffic in urban environments, volume transmission in the brain and communication through online social networks.

1 Introduction

“The Target Problem” seems to be an easy problem when it deals with searching strategies toward an efficient target identification on a networked environment. This environment can be represented by the discrete space created by a graph $G = (V, E)$, in which a set of vertices V are interconnected by pairs forming a set of edges E [25]. Therefore, once a target has been identified in the graph, e.g., the vertex $w \in V$, our task can be thought to be reduced to find the shortest topological path connecting our current location, e.g., the vertex $v \in V$, with the target. A path refers to a sequence of different vertices and edges between two corresponding vertices.

Ernesto Estrada
Institute for Cross-Disciplinary Physics and Complex Systems (IFISC), CSIC-UIB, Palma de Mallorca, Spain, e-mail: estrada@ifisc.uib-csic.es

Among all existing paths between two vertices, the one having the minimum length, in terms of the number of edges in the path, is the shortest path. There are several algorithms for finding the shortest path between two vertices in a graph [48,92,100]. The Bellman-Ford-Moore algorithm [7,40,77] allows to find the shortest paths from the source vertex to all other vertices in a graph in which edges can be weighted by positive numbers. The algorithm has a time complexity of $O(V \cdot E)$, which because $\#E \geq \#V - 1$ in connected graphs, makes the complexity relatively large, i.e., in general larger, than $O(V^2)$. The most popular algorithm for finding shortest paths is the Dijkstra algorithm [20], which finds the shortest paths from the source vertex to all other vertices in the graph with time complexity $O(V^2)$. Finally, the Floyd-Warshall algorithm [39,93] finds the shortest paths between all pairs of vertices in a graph in $O(V^3)$ allowing weights in the edges, which can be positive or negative.

Let us now see the target problem from the perspective of a single vertex in a network representation of a complex system [31]. Think for instance about a neuron which is interconnected to others in a human brain composed by about 10^{10} neuronal cells and 10^{14} interconnections [64]. Can this single neuron find the shortest path to a target neuron in this network? If the neuron is going to use a routing/navigation process to find the shortest path to a specific target it needs to have a “global knowledge about the network topology” [50]. This is exactly what the previously mentioned algorithms use: global information about the network. It is hard to digest that every single neuron has a map of the 86 billion neurons in the brain. In spite of this, there are authors who believe that [68] “the shortest path plays an important role in the information transmission of a brain network, and it is a very important measure to describe the internal structure of the brain network”. The claim is mainly based on the apparent fact that “the shortest path can transmit the information more quickly and reduce brain consumption” [68]. For such a thing to be possible it is necessary that there exists a central controller with “global knowledge about the network topology” [50] to direct the information through the shortest paths connecting pairs of brain regions. But even in this “mystical” scenario, the use of the shortest path could be inefficient from an energetic point of view. Tomasi et al. [90] have found experimentally that “a higher degree of connectivity was associated with nonlinear increases in metabolism”. That is, the more connected a vertex is, the higher its energy consumption. It is evident that a highly connected vertex supports many shortest paths crossing it—a vertex of degree k may support up to $k(k-1)/2$ shortest paths of length two between its nearest neighbors, apart from the rest. Therefore, it is not necessarily true that the use of shortest paths “reduces brain consumption” as claimed in [68].

How is then possible that information finds its way from a specific source to a specific target in such complex networked environments like a human brain? Diffusion may be a plausible solution. At the end, a diffusive process can transmit information between a source and a target without any “knowledge about global network topology” [50]. This strategy will also avoid the problem of increasing glucose consumption because it “prevents particles or messages from taking shortest paths” [50]. Diffusion is ubiquitous in nature and in many man-made systems, even in those in which it seems to be counterintuitive [72]. For instance, when navigating a city at rush

hour, drivers in general know the shortest topological paths between origin-target pairs. However, it has been seen statistically that they frequently avoid such paths for several reasons [3]. The first is that such routes contain, with high probability, highly interconnected intersections. Therefore, traveling through shortest topological paths necessarily would imply more complicated maneuvers and more waiting time due to traffic signals, jams, etc. The second is that in navigating between origin-target pairs, drivers frequently use their own “cognitive maps”, which allow them “establishing locations, understanding distances between locations, comprehending the direction of one location from another, linking locations in sequence, and transferring knowledge from the mental arena to the surrounding physical environment” [49]. We can think that every driver in the same city has his own cognitive map to go from one place to another, particularly at rush hour. Indeed, Golledge and Gärling [49] have found, in travel-related literature, more than 20 different strategies used by drivers to find their routes. Their search include reports in fields such as travel behavior, operations research, transport geography, and behavioral travel modeling. Such mental algorithms include strategies like: using the “longest leg first”, or using the “shortest leg first”, selecting the route that has “fewest turns”, or “fewest lights or stop signs”, or “fewest obstacles or obstructions”, etc. If we assign randomly and independently these algorithms to the drivers in a city at rush hour, what we will observe are patterns similar to those of a diffusive motion [3, 61, 98].

When we talk about diffusion we typically talk about a series of different physical phenomena, which include classical conservative diffusion, non-conservative diffusion, and anomalous diffusion (sub- and superdiffusion) [18, 46, 60, 66, 84]. By conservative we mean that the amount of diffusive particles is constant in the graph, while in a non-conservative diffusion the number of diffusive particles can change with time. The reason for the latest is that some particles are created/annihilated in the graph, maybe because they escape to the environment in which this graph is embedded. Here, we study the similarities and differences between conservative and non-conservative diffusion on graphs. We discover here that the non-conservative diffusive strategy present certain advantages for a single vertex in a network to send information to a target in a faster way relative to the conservative one. The main reason behind this advantage of non-conservative diffusion over the conservative one resides in the trajectories that diffusive particles follow in both processes. These trajectories are found here by means of a geometrization of the graphs using the Euclidean distances induced by the diffusive processes. We find here that non-conservative diffusive particles follow trajectories involving low-connected vertices, which coincide with the bypasses recently found to play an important role in complex networks navigation [33], while the conservative ones can follow trajectories more similar to those of the shortest topological paths. We finalize this chapter with some examples of complex systems in which such non-conservative diffusive strategies are used.

2 The setting

Here we only consider simple, undirected and unweighted graphs $G = (V, E)$, where $V = \{v_1, \dots, v_n\}$ is the set of vertices with $\#V = n$, and $E = \{(v_i, v_j) \mid v_i, v_j \in V\}$ is the set of edges with $\#E = m$. We use indistinctly the terms graphs and networks to refer to G , although the term “network” is mainly reserved to the skeleton of complex systems in the real-world. The terms vertex and node are also used indistinctly.

A walk of length l in a graph is a sequence of (not necessarily different) vertices $v_1, v_2, \dots, v_l, v_{l+1}$ such that for each $i = 1, 2, \dots, l$ there is an edge from v_i to v_{i+1} . The walk is known as closed if $v_{l+1} = v_1$. If all the vertices and edges of the walk are different we say that it corresponds to a path. Among all the paths that connect a pair of vertices, the one having the minimum length is the shortest path. The shortest path between two vertices is a distance. A graph for which there is at least a path between every pair of vertices is said to be connected. We will consider here only connected graphs.

Two vertices are adjacent in the graph if they share a common edge. Then the square symmetric matrix A , whose entries are defined as

$$A_{i,j} = \begin{cases} 1 & (i, j) \in E \\ 0 & (i, j) \notin E, \end{cases} \quad (1)$$

represents the adjacency between pairs of vertices in the graph and it is known as the adjacency matrix.

The following is a very well-known result (see for instance [8]):

Theorem 1 Let G be a simple connected graph. Then, the (i, j) entry of the l th power of A , $(A^l)_{ij}$, counts the number of walks of length l between the vertices i and j . \square

The number of vertices adjacent to a vertex i is known as the degree of i and denoted by k_i . The diagonal matrix K of the degree of the vertices in G is known as the degree matrix. Then, the matrix $L = K - A$ is defined as the graph Laplacian matrix of G , see further for a “first-principles” definition.

3 Normal diffusion

Let us consider a simple undirected graph as the one illustrated in Fig. 1 in which there is a “concentration” $C_i(0) = C_i(t=0) \in \mathbb{R}_+ \cup \{0\}$ of a given “item” at the node i at a time $t = 0$.

At every edge (i, j) there will be a gradient $C_i(0) - C_j(0)$ of concentrations. As time evolves, there is a “movement” of the “items” from high concentration to low concentration. Let us pick a vertex of G , let say A , and analyze how the concentration of the items at this vertex changes in time. Because A is connected to B and to C we have that the change of concentration at A is proportional to the sum of the gradients with both B and C :

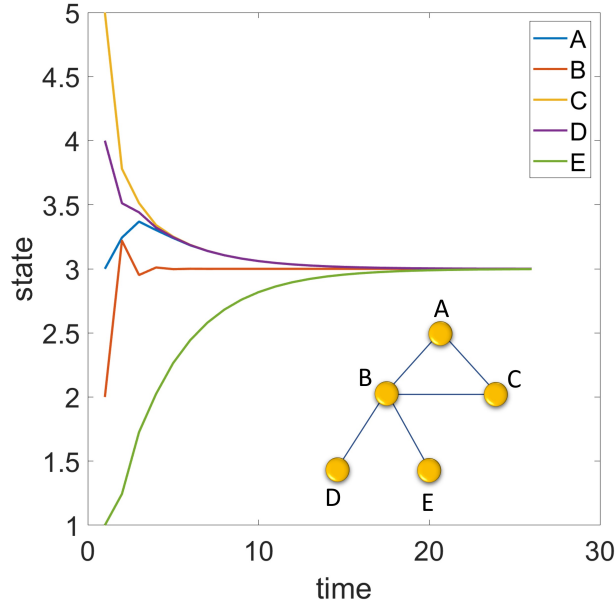


Fig. 1: Illustration of the time-evolution of the standar diffusion on the graph illustrated in the inset, when the intial concentrations at the vertices is given by: $C^0 = [3, 2, 5, 4, 1]^T$ for the vertices $V = \{A, B, C, D, E\}$.

$$\frac{dC_A(t)}{dt} = \gamma [(C_B(t) - C_A(t)) + (C_C(t) - C_A(t))], \quad (2)$$

where γ is a proportionality coefficient known as diffusivity or diffusion coefficient [46]. We can rearrange this equation for the node A as:

$$\frac{dC_A(t)}{dt} = \gamma [C_B(t) + C_C(t) - 2C_A(t)], \quad (3)$$

where $C_B(t) + C_C(t)$ is the sum of the concentrations at the nearest neighbors of A and $2C_A(t)$ is the concentration at A multiplied by the number of nearest neighbors it has, i.e., its degree. Let us hereafter consider $\gamma = 1$. Then, we can write generically the following equation:

$$\dot{C}_i(t) = \left(\sum_{(j,i) \in E} C_j(t) \right) - k_i C_i(t), \quad (4)$$

where k_i is the degree of vertex i . It is worth mentioning here that this equation is a particular case of the so/called “master equation”, which is considered in other Chapters of this book.

Let us now defined the following.

Definition 2 Let $\mathcal{H} := \ell^2(V)$ be a Hilbert space and let $f \in \mathcal{H}$ be a function. Then, the adjacency operator \mathcal{A} of G is defined as [70]:

$$(\mathcal{A}f)(v) := \sum_{(w,v) \in E} f(w). \quad (5)$$

Notice that if G is infinite but locally finite, i.e., $k_i < \infty$ for all vertices of G , the adjacency operator is a bounded selfadjoint operator in \mathcal{H} [70]. If the graph is finite the adjacency operator coincides with the adjacency matrix A of the graph.

Definition 3 Let $\mathcal{H} := \ell^2(V)$ be a Hilbert space and let $f \in \mathcal{H}$ be a function. Then, the degree operator \mathcal{K} of G is defined as:

$$(\mathcal{K}f)(v) := k_v f(v). \quad (6)$$

If the graph is finite the degree operator is realized by the diagonal matrix K of vertices degrees of the graph.

Let $\dot{C}(t) := [\dot{C}_{v_1}(t) \dots \dot{C}_{v_n}(t)]^T$ and let $C(t) := [C_{v_1}(t) \dots C_{v_n}(t)]^T$. Then, we can write the set of diffusion equations for all the vertices of the graph in the following matrix-vector form:

$$\begin{aligned} \dot{C}(t) &= AC(t) - KC(t) \\ &= (A - K)C(t) \\ &= -LC(t), \end{aligned} \quad (7)$$

where $L := K - A$ is the Laplacian of the graph, which can be formally defined as:

Definition 4 Let $\mathcal{H} := \ell^2(V)$ be a Hilbert space and let $f \in \mathcal{H}$ be a function. The Laplacian operator \mathcal{L} of G is defined as [53]:

$$(\mathcal{L}f)(v) := \sum_{(w,v) \in E} (f(w) - f(v)). \quad (8)$$

When the graph is finite, then L is the matrix representation of this operator. \square

We then have the diffusion equation of the graph as:

$$\dot{C}(t) = -LC(t) \quad (9)$$

where $L := K - A$ is the graph Laplacian and K is a diagonal matrix of vertex degrees, and where the initial condition is $C(0) = C^0 \in \mathbb{R}_+^{n \times 1} \cup \{0\}$.

3.1 Some properties of L

Here we state some of the general properties of the graph Laplacian matrix L (see [54, 55, 73, 76]).

Definition 5 Let m be the number of edges and n be the number of vertices. Then the incidence matrix ∇ is the $m \times n$ matrix given by:

$$\nabla_{v,e} = \begin{cases} -1, & e = (v, w) \text{ and } v > w \\ 1, & e = (v, w) \text{ and } v < w \\ 0, & \text{otherwise.} \end{cases} \quad (10)$$

Lemma 6 The Laplacian matrix of the graph L is given by

$$L = \nabla^T \nabla, \quad (11)$$

such that the incidence matrix can be considered as a gradient matrix of a graph where concentrations are arbitrarily fixed at the nodes. \square

The following describes some of the general properties of the Laplacian.

Theorem 7 The Laplacian matrix L of a graph: \square

1. is a positive semidefinite matrix, indeed $f^T L f = \sum_{(v,w) \in E} (f(v) - f(w))^2 \geq 0$;
 - a. always has an eigenvalue equal to 0;
 - b. the multiplicity of the zero eigenvalue is equal to the number of connected components of the graph.

3.2 Conservative nature of the graph diffusion

Definition 8 A diffusion process is said to be conservative if the number of diffusive particles is constant along the time. That is, if and only if $\mathbf{1}^T C(t) = \mathbf{1}^T C^0$ for any $0 \leq t \leq \infty$. Otherwise the process is said to be non-conservative \square

Lemma 9 The diffusion (9) on a connected graph is always conservative. \square

Proof The solution of the diffusion equation is:

$$C(t) = e^{-tL} C^0. \quad (12)$$

Let us take the sum of the entries of $C(t)$ at an arbitrary time t ,

$$\mathbf{1}^T C(t) = \mathbf{1}^T e^{-tL} C^0 \quad (13)$$

and let us expand the matrix exponential in its Taylor series

$$\mathbf{1}^T C(t) = \mathbf{1}^T C^0 - t \mathbf{1}^T L C^0 + \frac{t^2}{2!} \mathbf{1}^T L^2 C^0 + \dots + \left(\frac{(-1)^k t^k}{k!} \right) \mathbf{1}^T L^k C^0 + \dots \quad (14)$$

Because L is positive semidefinite, we have that $\mathbf{1}^T L = 0$ and so $(\mathbf{1}^T L) L^{k-1} = 0$, so that $\mathbf{1}^T C(t) = \mathbf{1}^T C^0$ for any t . \square

In plain words, the previous result means that at any time t the sum of concentrations of particles at the nodes of the graph is exactly the same, independently of t .

Let us now see what is the steady state of the diffusive dynamics in a graph.

Lemma 10 Let C_i^0 be the state of the vertex i at time $t = 0$. Then, when $t \rightarrow \infty$ the solution of the diffusion equation of the graph converges to $C_i(t \rightarrow \infty) = \frac{1}{n} \sum_{i=1}^n C_i^0$, i.e., to the average of the state of nodes in the initial condition. The rate of convergence of the diffusion is dictated by the smallest nontrivial eigenvalue of L . \square

Proof Let $0 = \mu_1 < \mu_2 \leq \dots \leq \mu_n$ be the eigenvalues of L and let φ_i the orthonormalized eigenvector associated with μ_i . Then, we can write

$$\begin{aligned} C(t) &= e^{-tL} C^0 \\ &= \varphi_1 e^{-t\mu_1} (\varphi_1^T C^0) + \varphi_2 e^{-t\mu_2} (\varphi_2^T C^0) + \dots + \varphi_n e^{-t\mu_n} (\varphi_n^T C^0). \end{aligned} \quad (15)$$

When t is sufficiently large we have

$$\begin{aligned} \lim_{t \rightarrow \infty} C(t) &= \varphi_1 e^{-t\mu_1} (\varphi_1^T C^0) \\ &= \frac{1}{\sqrt{n}} \mathbf{1} \left(\frac{1}{\sqrt{n}} \mathbf{1}^T C^0 \right) \\ &= \mathbf{1} \left(\frac{1}{n} \sum_{i=1}^n C_i^0 \right), \end{aligned} \quad (16)$$

which proves the first part of the result. Because μ_2 is the second smallest eigenvalue of L , it will dictate the rate of convergence of the process. \square

3.3 Intuition of the conservative diffusion on graphs

We start here by writing an iterative form of the diffusion dynamics on graphs in discrete-time:

$$C_i(r+1) = C_i(r) - \varepsilon C_i(r) k_i + \varepsilon \sum_{(j,i) \in E} C_j(r), \quad (17)$$

where $\varepsilon > 0$ is the step-size. If we introduce the following matrix $P := I - \varepsilon L$, which was proposed to be called the Perron matrix by Olfati-Saber et al. [79], we can write the discrete-time diffusion dynamics as:

$$C(r+1) = PC(r). \quad (18)$$

This formulation allows us to interpret what is happening in the diffusive process on a graph in a step-by-step basis. That is, if the “concentration” of an item at the vertex i at time step r is equal $C_i(r)$, then the node i will transfer the amount $\varepsilon C_i(r)$ to every of its nearest neighbors at time step $r+1$, at the same time that it will receive $\varepsilon C_j(r)$ from every of its j th nearest neighbors. This means that at every time step there is a trade off in which pairs of connected vertices interchange concentrations between each other, but such a process goes in the direction of lower concentration.

Let us explain this with an example based on the graph illustrated in Fig. 1. Let us consider the following initial condition: $C^0 = [3, 2, 5, 4, 1]^T$. That is, the vertex A , which is connected to vertices B and C , has an initial concentration of $C_A^0 = 3$. At the next time step, $r = 1$, A will transfer to B the amount $\varepsilon C_A^0 = 3\varepsilon$ and will receive from B the amount $\varepsilon C_B^0 = 2\varepsilon$. This means that the net balance of A for its tradeoff with B is: $C_{A\rightleftharpoons B}(1) = -3\varepsilon + 2\varepsilon = -\varepsilon$, which implies that A has transferred more to B than what it has received from that vertex. If we do the same analysis for the tradeoff between A and C , which has initial concentration 5, we have: $C_{A\rightleftharpoons C}(1) = -3\varepsilon + 5\varepsilon = 2\varepsilon$, clearly indicating that A receives more from C than what it transfers to that node. Because A is connected only to B and C , we have: $C_A(1) = C_A^0 + C_{A\rightleftharpoons B}(1) + C_{A\rightleftharpoons C}(1) = 3 - \varepsilon + 2\varepsilon = 3 + \varepsilon$, indicating that in the first step A increases its concentration in spite of the fact that it has transferred more to B than what it has received from it, but such a loss is compensated by the gains from C which has a high initial concentration. The process continues with these “negotiations” of concentrations between pairs of connected vertices so that the steady state is eventually reached as illustrated in Fig. 1. This kind of negotiation is the main reason why this process is known in engineering as the “consensus protocol” (see for instance [74]).

4 Non-conservative diffusion

Let us consider the following matrix: $\mathcal{L}_\chi := \chi I - A$, which was first analyzed in [44] (see also [45]) and we propose here to call it the Lerman-Ghosh Laplacian of a graph. Let us then consider the following diffusive process

$$\dot{C}(t) = -(\chi I - A)C(t) = -\mathcal{L}_\chi C(t). \quad (19)$$

At the local level, the concentration of items at a vertex i at time t is given by

$$\dot{C}_i(t) = \left(\sum_{(i,j) \in E} C_j(t) \right) - \chi C_i(t). \quad (20)$$

We now analyze the solution of this dynamics. Let $\lambda_1 > \lambda_2 \geq \dots \geq \lambda_n$ be the eigenvalues of the adjacency matrix of a simple, connected graph G , and let ψ_j be the (orthonormalized) eigenvector associated with λ_j . Then, we have the following result.

Theorem 11 Let $\mathcal{L}_\chi = \chi I - A$ be the Lerman-Ghosh Laplacian and let

$$\dot{C}(t) = -\mathcal{L}_\chi C(t) \quad (21)$$

with initial condition $C(t) = C_0$. Then,

$$\lim_{t \rightarrow \infty} C(t) = \begin{cases} (\psi_1^T C^0) \psi_1 e^{t(\lambda_1 - \chi)} = \infty \text{ for } \chi < \lambda_1 \\ \left(\sum_j C_j^0 \psi_1(j) \right) \psi_1 \text{ for } \chi = \lambda_1 \\ (\psi_1^T C^0) \psi_1 e^{-t(\chi - \lambda_1)} = 0 \text{ for } \chi > \lambda_1. \end{cases} \quad (22)$$

Proof The solution of the diffusion equation is given by

$$C(t) = e^{-t(\chi I - A)} C^0, \quad (23)$$

which can be written as

$$C(t) = e^{t(\lambda_1 - \chi)} (\psi_1^T C^0) \psi_1 + e^{t(\lambda_2 - \chi)} (\psi_2^T C^0) \psi_2 + \dots + e^{t(\lambda_n - \chi)} (\psi_n^T C^0) \psi_n. \quad (24)$$

Then, when $\chi < \lambda_1$ we have

$$\lim_{t \rightarrow \infty} C(t) = e^{t(\lambda_1 - \chi)} (\psi_1^T C^0) \psi_1, \quad (25)$$

which diverges as $t \rightarrow \infty$.

If $\chi = \lambda_1$ we have that the first term of Eq. (24) is zero, and the rest are negative, such that

$$\lim_{t \rightarrow \infty} C(t) = (\psi_1^T C^0) \psi_1, \quad (26)$$

which indicates that the solution is proportional to the entries of the eigenvector ψ_1 associated with the spectral radius λ_1 of A . This eigenvector was introduced by Bonacich [9–11] as a centrality index of the vertices in a graph and it is nowadays known as the eigenvector centrality. Therefore, the current framework provides a dynamics interpretation of this centrality index in term of the concentration reached by a vertex at the steady state of a non-conservative diffusion controlled by the Lerman-Ghosh Laplacian matrix when $\chi = \lambda_1$. Because the second smallest eigenvalue of $(\lambda_1 I - A)$ is $\lambda_1 - \lambda_2$, it determines the rate of convergence of the diffusive process. Notice that if $C^0 = \psi_1$, then the diffusion process is conservative because:

$$\mathbf{1}^T C(t) = [\mathbf{1}^T \psi_1] = \mathbf{1}^T C^0. \quad (27)$$

Finally, if $\chi > \lambda_1$ then,

$$\lim_{t \rightarrow \infty} C(t) = e^{-t(\chi - \lambda_1)} (\psi_1^T C^0) \psi_1, \quad (28)$$

which goes to zero as $t \rightarrow \infty$.

Corollary 12 Let G be a regular graph, i.e., a graph in which all vertices have the same degree. Then, the diffusion model (19) with $\chi = \lambda_1$ is conservative for any initial condition, where $\lim_{t \rightarrow \infty} C_i(t) = \frac{1}{n} \sum_j C_j^0$ for all $j \in V$. If the graph is not regular, the diffusion process with $\chi = \lambda_1$ and $C^0 \neq \psi_1$, is non-conservative. This is because $\psi_1(j) < 1$ and then $\lim_{t \rightarrow \infty} C(t) = \left(\sum_j C_j^0 \psi_1(j) \right) \psi_1 < \frac{1}{n} \sum_j C_j^0$ such that $0 < C(t \rightarrow \infty) < C^0 < \infty$. The exception is when $\psi_1(j) = \frac{1}{\sqrt{n}}$ for all $j \in V$, which is the case of the regular graph. \square

Remark 13 The diffusion process (19) is non-conservative for all values of χ and initial conditions C^0 , except for the specific case in which $\chi = \lambda_1$ and $C^0 = \psi_1$. \square

In Fig. 2 we illustrate the three examples of non-conservative diffusion modeled by Eq. (19) using the Lerman-Ghosh Laplacian for the graph and initial condition of Fig. 1 with $\chi < \lambda_1$ (a), $\chi = \lambda_1$ (b) and $\chi > \lambda_1$ (c). Notice that when $\chi = \lambda_1$ and $C^0 \neq \psi_1$ the process can be said to be quasi-conservative as the number of particles when $t \rightarrow \infty$ is just a bit smaller than at $t = 0$.

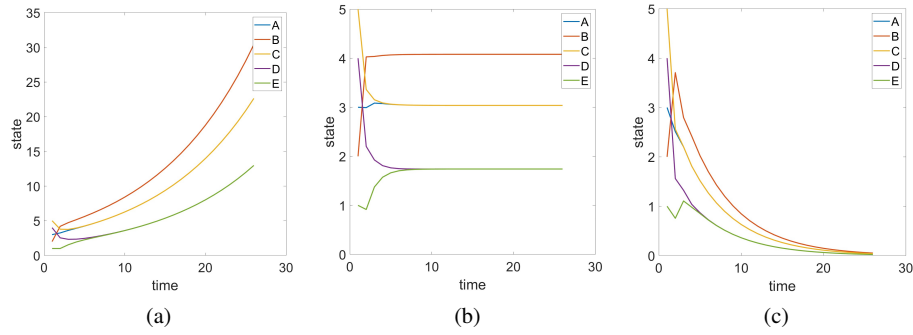


Fig. 2: Illustration of the non-conservative diffusion process on the graph illustrated in Fig. 1 for $\chi < \lambda_1$ (a), $\chi = \lambda_1$ (b) and $\chi > \lambda_1$ (c).

4.1 On the intuition of the non-conservative diffusion

In the discrete time setting Eq. (19) indicates that the resulting concentration at every vertex of the graph at the discrete time step $r + 1$ is given by

$$C_i(r+1) = C_i(r) - \varepsilon \chi C_i(r) + \varepsilon \sum_{(j,i) \in E} C_j(r). \quad (29)$$

If we introduce the following matrix $Q := I - \varepsilon(\chi I - A) = (1 - \varepsilon\chi)I + A$, then we can write the discrete-time diffusion dynamics as:

$$C(r+1) = QC(r). \quad (30)$$

In order to gain intuition on what is happening let us start by considering that a graph is connected to a given reservoir in which there could be an infinite reserve of the item to be diffused across the graph. Every vertex of the graph is connected to the reservoir by means of a semi-edge, which has one endpoint at the vertex, and the other one is freely dangling in the reservoir. We then consider a two-step diffusion process as follows. First every vertex i expels $\varepsilon\chi C_i(r)$ to the reservoir, where χ is a constant such that $\varepsilon\chi \leq \max_i C_i^0$ to guarantee that no vertex is left with a negative concentration. This first step creates a pool of the item being diffused in the reservoir which adds to the existing reserve of items in the reservoir (in case it exists). In the second step of the process every vertex sucks from the reservoir an amount equal to $\varepsilon \sum_{(j,i) \in E} C_j(r)$.

For instance, let us consider the graph of Fig. 1, which has $\lambda_1 \approx 2.343$, and let us use $\chi = 3$ and $\varepsilon = 0.25$ as before. Then, vertex A expels $\varepsilon\chi C_A^0 = 2.25$ of its initial concentration to the reservoir. The amounts expelled by the other vertices are: 1.5; 3.75; 3.0; 0.75. In total, the vertices have expelled 11.25 of its initial total concentrations that sum 15. At every vertex remains a concentration equal to: 0.75; 0.50; 1.25; 1.0; 0.25, respectively, as can be seen in Fig. 3(a). In the second step, vertex A has to suck $\varepsilon \sum_{(j,A) \in E} C_j^0 = 1.75$, while the others will suck: 3.25; 1.25; 0.50; 0.50; respectively, for a total of 7.25. This amount to be sucked from the reservoir is smaller than the one expelled previously to it. Therefore, in the reservoir there will remain $11.25 - 7.25 = 4$, and the sum of the concentrations at the nodes will be 11 instead of the 15 that there was initially. This is illustrated in Fig. 3(b). The repetition of this process makes that the vertices get empty as time evolves because in every time step there are more “items” deposited in the reservoir than the ones extracted from it. Notice that in this case the reservoir at $t = 0$ may be empty. Here, the reservoir is just a virtual space used to gain an intuition on how the Kerman-Ghosh Laplacian operates over a diffusive process on the graph. More physically realistic scenarios can be adapted according to specific situations. It is worth mentioning that this description suggests that a reservoir can be introduced as an additional sink or source node to the graph, which is connected to all other nodes. It has been shown that accounting for asymmetric transition rates (from and to the reservoir) requires the use of transition matrices, see, e.g., [52] and references therein. We show here that the Lerman-Ghost Laplacian represents an interesting alternative way to describe sink/source nodes in graphs.

If $\chi < \lambda_1$ the amount $\varepsilon\chi C_i(r)$ expelled by the vertices to the reservoir is smaller than the amount $\varepsilon \sum_{(j,i) \in E} C_j(r)$ that the vertex has to suck from the reservoir. For instance if we use $\chi = 1$, the vertices will expel in total 3.75 to the reservoir as illustrated in Fig. 4(a). However, the vertices have to extract 7.25 from the reservoir, which means they will take the 3.75 previously expelled plus 3.5 from the reserve in the reservoir. Here the total amount at the vertices at $t = 1$ is 19 (see Fig. 4(b))

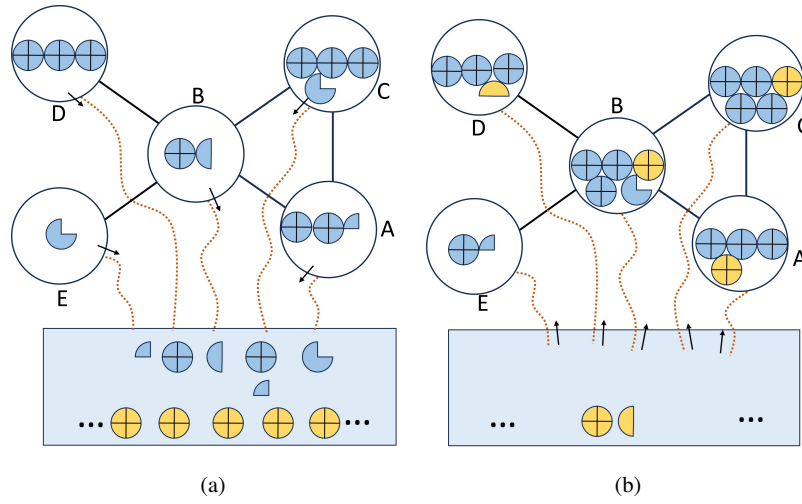


Fig. 3: Schematic representation of the non-conservative diffusive process when $\chi > \lambda_1$.

instead of the amount equal to 15 which existed at $t = 0$. The consequence of the repetition of this process is that the concentrations at the vertices grows to infinity as time evolves due to the fact that vertices extract more “items” from the reservoir than the ones they previously expel to it.

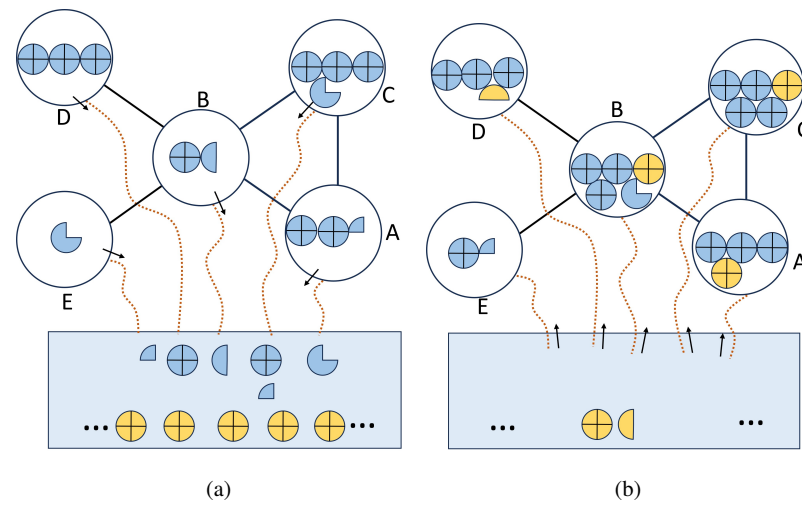


Fig. 4: Schematic representation of the non-conservative diffusive process when $\chi < \lambda_1$.

5 Logistic diffusion

It is certainly unrealistic to think about systems in which a non-conservative diffusion blows up when $t \rightarrow \infty$. This situation is avoided in the so-called reaction-diffusion models, where we allow that the vertices create or annihilate items to avoid that their concentrations go to zero or to infinity:

$$\dot{C}(t) = -LC(t) + f(C(t)). \quad (31)$$

An example of this model is the Fisher-Kolmogorov-Petrovsky-Piskunov [38, 62] (see also [21]) where $f(C(t)) = \alpha C(t) \left(1 - \frac{C(t)}{\mathcal{C}}\right)$ with α being the growth rate and \mathcal{C} being the carrying capacity. The model represents the linear growth of the particle population in proportion to its current size, and the negative quadratic one has the effect of curtailing the items population growth.

Let us here consider a general model of the form

$$\dot{C}(t) = -(\chi I - A)C(t) + f(C(t)), \quad (32)$$

such that although it is non-conservative it reaches a steady state in which the concentration at every vertex in the graph is equal. We consider the non-conservative diffusion with Lerman-Ghosh Laplacian, $\gamma = 1$, $\chi < \lambda_1$ and $C(0) = C^0$ with $0 \leq C_i^0 < 1$. Then, because the graphs considered here are never the trivial graph we have that $\lambda_1 > 0$, so that by setting $\chi = 0$ we always guarantee the condition that $0 = \chi < \lambda_1$. If we consider $f(C(t)) = 0$, the model $\dot{C}(t) = AC(t)$ always blows up because the adjacency operator sums the concentrations of the newest neighbors of every node, which continuously increases:

$$\dot{C}_i(t) = \sum_{(j,i) \in E} A_{ij} C_j(t). \quad (33)$$

We consider here that a fraction of the concentration increased at the vertex i is removed from the node to the reservoir. Because $C_i(t) < 1$ we consider that the fraction to be removed is equal to $C_i(t)$ multiplied by the amount in which the concentration has increased:

$$\dot{C}_i(t) = \sum_{(j,i) \in E} A_{ij} C_j(t) - C_i(t) \sum_{(j,i) \in E} A_{ij} C_j(t). \quad (34)$$

Obviously, we can regroup the terms to obtain:

$$\dot{C}_i(t) = (1 - C_i(t)) \sum_{(j,i) \in E} A_{ij} C_j(t), \quad (35)$$

which is nothing else than the logistic differential equation [6] (for applications see also [16, 56, 63, 99]).

The logistic model can be rewritten (see [1]) as

$$\frac{1}{1 - C_i(t)} \frac{dC_i(t)}{dt} = \sum_{(j,i) \in E} A_{ij} \left(1 - e^{-(-\log(1 - C_j(t)))} \right), \quad (36)$$

which is equivalent to

$$\frac{dy_i(t)}{dt} = \sum_{(j,i) \in E} A_{ij} f(y_j(t)), \quad (37)$$

where $y_i(t) := g(C_i(t)) = -\log(1 - C_i(t)) \in [0, \infty]$, $f(y) := 1 - e^{-y} = g^{-1}(y)$.

Lee et al. [65] have considered for a given C^0 an approximate solution $\hat{C}(t)$ to the logistic equation, which is given by $\hat{C}(t) = f(\hat{y}(t))$, where $\hat{y}(t)$ is the solution of the following linearized version of the previous nonlinear equation

$$\frac{d\hat{y}(t)}{dt} = \text{Adiag}(1 - C_0) \hat{y}(t) + b(C_0), \quad (38)$$

where $\text{diag}(1 - C_0)$ represents a diagonal matrix whose main diagonal entries are given by the values of $1 - C_0$ and the rest of entries are zero. Here, $\hat{y}_0 = g(C^0)$ and $b(C) := C + (1 - C) \log(1 - C)$, which can be considered as a reaction-diffusion equation on the new variable $\hat{y}(t)$. Let $a \leq b$ means that $a(i) \leq b(i)$ for all entries $i = 1, \dots, n$ of the two vectors a and b . We then reproduce the following result.

Theorem 14 [65] For any t it is true that $C(t) \leq \hat{C}(t)$ when they have the same initial conditions, and the solution of the linearized logistic model is \square

$$\begin{aligned} \hat{y}(t) &= e^{(t-t_0)\text{Adiag}(1-C^0)} g(C^0) \\ &+ \sum_{k=0}^{\infty} \frac{(t-t_0)^{k+1}}{(k+1)!} \left[\text{Adiag}(1-C^0) \right]^k Ab(C^0), \end{aligned} \quad (39)$$

which reduces to

$$\hat{y}(t) = g(C^0) + \left[e^{t\text{Adiag}(1-C^0)} - I \right] \text{diag}(1 - C^0)^{-1} C^0, \quad (40)$$

when $C^0 < \mathbf{1}$, and to

$$\hat{y}(t) = g(C^0) + \sum_{k=0}^{\infty} \frac{t^{k+1}}{(k+1)!} \left[\text{Adiag}(1 - C^0) \right]^k AC^0 \quad (41)$$

when $C_i^0 \in \{0, 1\}$.

Remark 15 Here we show that both solutions when $C^0 < \mathbf{1}$, and when $C_i^0 \in \{0, 1\}$ are the same. For that, let us consider $D = \text{diag}(1 - C^0)$ in the solution for $C_i^0 \in \{0, 1\}$. Then,

$$\begin{aligned}
\hat{y}(t) &= g(C^0) + t \sum_{k=0}^{\infty} \frac{[tAD]^k}{(k+1)!} AC^0 \\
&= g(C^0) + tE_{1,2}(A)AC^0 \\
&= g(C^0) + t \left(\frac{e^{tAD} - I}{tAD} \right) AC^0 \\
&= g(C^0) + \left(\frac{e^{tAD} - I}{D} \right) C^0,
\end{aligned} \tag{42}$$

which is the solution for $C^0 < \mathbf{1}$. We have used the definition of the Mittag-Leffler matrix function:

$$E_{\alpha,\beta}(M) := \sum_{k=0}^{\infty} \frac{M^k}{\Gamma(\alpha k + \beta)}, \tag{43}$$

where M is a matrix, which for $\alpha = 1$ and $\beta = 2$ is

$$E_{1,2}(M) := \sum_{k=0}^{\infty} \frac{M^k}{\Gamma(k+2)} = \sum_{k=0}^{\infty} \frac{M^k}{(k+1)!} = \frac{e^M - I}{M}, \tag{44}$$

where I is the identity matrix. This specific Mittag-Leffler matrix function [5, 29, 43] is also known as the Ψ -matrix function (see Section 10.7.4 in [57]). Notice that $E_{1,1}(M) = \exp(M)$.

Hereafter, we consider the realistic scenario in which the initial concentration of the item under study at one given vertex i is very small $C_i^0 \ll 1$, and zero elsewhere. In this scenario, $D \approx I$ and the solution of the approximate logistic diffusion equation is \square

$$\hat{y}(t) \approx e^{tA}C^0 - \left(C^0 + \log(1 - C^0) \right), \tag{45}$$

and

$$\hat{x}(t) = 1 - e^{-\hat{y}(t)}. \tag{46}$$

For instance, we illustrate in Fig. 5 the temporal evolution of this diffusion model on the simple graph of Fig. 1 with both the approximate and exact solutions.

Obviously,

$$\lim_{t \rightarrow \infty} \hat{y}(t) = e^{t\lambda_1} \left(\psi_1^T C^0 \right) \psi_1 - \left(C^0 + \log(1 - C^0) \right) = \infty, \tag{47}$$

such that

$$\lim_{t \rightarrow \infty} \hat{x}(t) = \mathbf{1}, \tag{48}$$

implying that the process is non-conservative as $\mathbf{1}^T C^0 = C_i^0 \ll 1$, and $\mathbf{1}^T C(\infty) = n$.

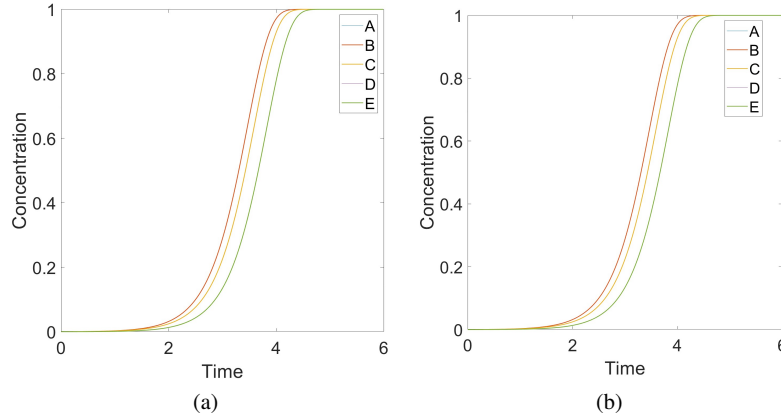


Fig. 5: Illustration of the time evolution of the logistic diffusion on the graph of Fig. 1 using the approximation eq. (45) instead of the exact solution of eq. (40). Here $C_A^0 = 0.001$ and $C_i^0 = 0$ for $i = \{B, C, D, E\}$.

6 Sending “information” to a target

In order to compare the two diffusion processes considered here, conservative and non-conservative ones, we select a graph formed by two cliques, which are interconnected by a path. Although these graphs are closely related to the so-called dumbbell graphs, they are not exactly the same, so we propose here to call them weight-lifting (WL) graphs. In Fig. 6 we illustrate the WL graph with two cliques of 10 vertices interconnected by a path of the same size.

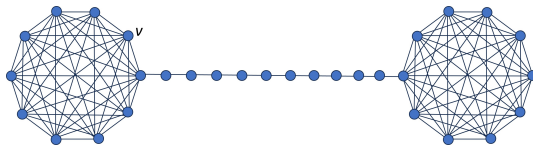


Fig. 6: Illustration of a WL graph formed by two cliques of 10 vertices interconnected by a path of the same size. A vertex which is in the clique but not in the path is denoted by v .

This kind of graphs is a good example of a difficult networked environment in which a particle in one of the cliques have to diffuse to find a target in the other clique. While it is relatively easy for a diffusive particle to navigate one of the cliques, it is more difficult to find the only path communicating the two cliques to move to the other. The WL graph built here has 10 vertices in each clique and 10 vertices in the path connecting them. Thus, we will call it $WL(10)$. In Fig. 7(a) we illustrate the

temporal evolution of the conservative diffusion of a concentration initially located in a clique vertex i different from the one connecting the clique to the path, such that $C_i^0 = 0.001$ and $C_j^0 = 0$ for all $j \neq i$. For the sake of comparison we illustrate in Fig. 7(b) the same process in an Erdős-Rényi random graph [22] having the same number of vertices and edges as the $WL(10)$ one. That is, this is a graph in which the difficulties inherent to the structure of the WL graph have been changed by an environment in which the particle can navigate in an easier way, although having the same number of vertices and edges. As can be seen in Fig. 7 the conservative diffusion takes about 100 times more time to reach the steady state in the dumbbell graph than in its random analogous.

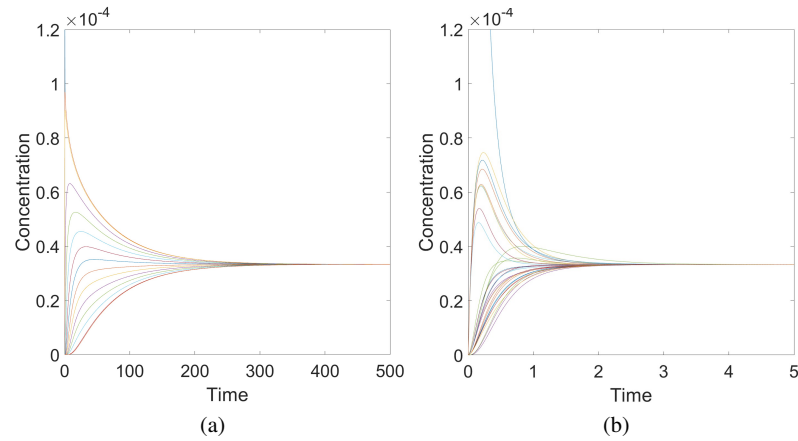


Fig. 7: Time evolution of conservative diffusion dynamics on a WL graph (a) with two cliques of 10 vertices interconnected by a linear chain of 10 vertices, and in the random graph (b)–of the Erdős-Rényi type– having the same number of vertices and edges like the graph in (a).

Let us now consider what happens with the non-conservative diffusion. To consider a process in which a steady state is reached we will use the non-conservative logistic diffusion equation on graphs using the approximation of Lee-Tenneti-Eun and the same initial condition as before.

It is remarkable to notice that the non-conservative diffusion only takes about two times more time to reach the steady state in the WL graphs than in its random analogous. This is illustrated in Fig. 8. If we compare this non-conservative process with the conservative one in the WL graph we observe that the first is about 100 times faster than the second one.

In Fig. 9 we illustrate the differences in the way in which the concentration of items is diffused from a vertex of the WL graph to the rest of the vertices. In this case we selected a vertex of the linear chain which is located close to the center (the linear chain has 10 vertices, and the vertex selected has four vertices to the right and five

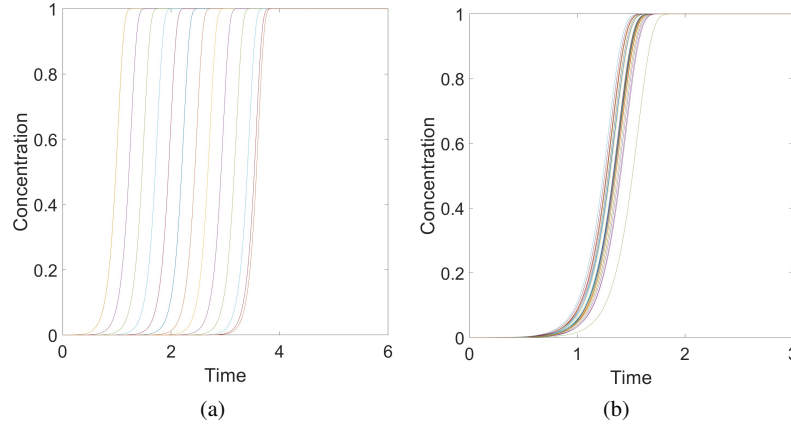


Fig. 8: Time evolution of non-conservative logistic diffusion dynamics on a WL graph (a) with two cliques of 10 vertices interconnected by a linear chain of 10 vertices, and in the random graph (b)—of the Erdős-Rényi type—having the same number of vertices and edges like the graph in (a).

to the left). At very short times, as illustrated in Fig. 9(a), it is already seen that the logistic diffusion spreads faster the concentration of items to the nearest neighbors of the central vertex than the standard diffusion. The main fundamental difference between the two dynamics occurs when the time advances. The standard diffusion evolves by flattening the peak of concentration at the central node while spreading the concentration from the closest to the farthest vertices (see 9(b)). The logistic diffusion progresses by extracting concentration from the central vertex and filling the two cliques at its expense. That is, it evolves by emptying the vertex in which the whole concentration is initially located and its nearest neighbors to fill the two cliques. Once the cliques are filled, as illustrated in Fig. 9(c), the central vertex and its nearest neighbors are filled again. This mechanism is possible only because the process is non-conservative and the vertices can “extract” concentration from the reservoir. The result of the process is that it is faster than the standard diffusion as we have seen before.

7 Trajectories of “items” to a target

Both the conservative classical diffusion model and the non-conservative ones studied here have solutions in which the term depending on the structure of the network is: $\exp(\beta M)$, where β is a parameter usually depending on time and diffusion coefficient and where $M = \{-L, A\}$. Hereafter we will consider only the case $\beta = 1$ for

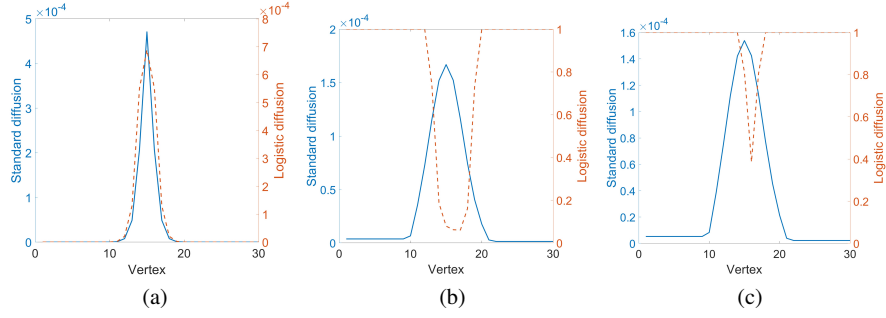


Fig. 9: Illustration of the time evolution of the diffusion through the $WL(10)$ graph with 30 vertices. The initial concentration is $C_i^0 = 0.001$ at a vertex close to the center of the linear chain connecting the two cliques. The dynamics is controlled by the standard diffusion equation (solid blue line) and by the logistic diffusion (broken red line). The plots are for $t = 0.5$ (a), $t = 3.0$ (b), and $t = 3.5$ (c).

the sake of simplicity. Let us focus on a couple of vertices designated by v and w . Then, at a given time the concentration at these nodes are:

$$C_v(t) = \sum_j (\exp(M))_{vj} C_j^0 \quad (49)$$

and

$$C_w(t) = \sum_j (\exp(M))_{wj} C_j^0. \quad (50)$$

Then, let

$$\mathcal{F}_{vw} |_{C_j^0 = \delta_{jv}} = C_v |_{C_j^0 = \delta_{jv}}(t) - C_w |_{C_j^0 = \delta_{jv}}(t), \quad (51)$$

be the diffusive flow from v to w in a graph when the initial concentration is totally located at the vertex v , $C_0(j) = \delta_{j,v}$, where $\delta_{i,j}$ is the Kronecker delta. Let us define the same in the other direction when the initial concentration is completely located at the vertex w ,

$$\mathcal{F}_{wv} |_{C_j^0 = \delta_{jw}} = C_w |_{C_j^0 = \delta_{jw}}(t) - C_v |_{C_j^0 = \delta_{jw}}(t). \quad (52)$$

7.1 Inducing a geometric embedding

Definition 16 Let $\mathcal{F}_{vw}|_{C_j^0=\delta_{jv}}$ and $\mathcal{F}_{wv}|_{C_j^0=\delta_{jw}}$ as defined previously. Then, let us define the sum of the gradients between the two nodes in both directions, which is given by: \square

$$\mathcal{D}_{vw}(M) := \mathcal{F}_{vw}|_{C_j^0=\delta_{jv}} + \mathcal{F}_{wv}|_{C_j^0=\delta_{jw}} = (\exp(M))_{vv} + (\exp(M))_{ww} - 2(\exp(M))_{vw}. \quad (53)$$

We then have the following result [23, 51, 81].

Proposition 17 $\mathcal{D}_{vw}(M)$ is a squared Euclidean distance between the pairs of vertices v and w . \square

Let us consider that $M = U^T \Lambda U$ where Λ is a diagonal matrix of eigenvalues of M and U is an orthogonal matrix of eigenvectors. Then, if φ_i is the i th column of U^T , we have

$$\begin{aligned} \mathcal{D}_{vw}(M) &= (\varphi_v - \varphi_w)^T e^\Lambda (\varphi_v - \varphi_w) \\ &= \left(e^{\Lambda/2} \varphi_v - e^{\Lambda/2} \varphi_w \right)^T \left(e^{\Lambda/2} \varphi_v - e^{\Lambda/2} \varphi_w \right) \\ &= (x_v - x_w)^T (x_v - x_w) \\ &= \|x_v - x_w\|^2. \end{aligned} \quad (54)$$

Definition 18 Let $s = \text{diag}(e^M)$. Then, we define the diffusion Euclidean Distance Matrix (EDM) as the matrix

$$\mathcal{M} = s \mathbf{1}^T + \mathbf{1} s^T - 2e^M. \quad (55)$$

An EDM is called [4, 59, 67, 87] spherical EDM or circum-EDM if the points p^1, p^2, \dots, p^n that generate the EDM lie on a hypersphere. Then, in the case of a graph, the points represent the vertices of the graph. If the corresponding EDM \mathcal{M} of the graph is circum-EDM it will immediately imply that the vertices of the graph can be embedded on the surface of a hypersphere such that the length of the chord separating two vertices v and w on the sphere is given by the corresponding Euclidean distance, which is the entry v, w of \mathcal{M} . We now prove that \mathcal{M} is indeed circum-Euclidean. \square

Proposition 19 \mathcal{M} is a circum-Euclidean distance matrix. \square

Proof We follow Gower [51] who proved that the points that generate the matrix M lie on the surface of a hypersphere if and only if $\mathbf{1}^T M^{-1} \mathbf{1} \neq 0$. Thus, we have to prove that M^{-1} exists. We first use the Sherman-Morrison-Woodbury formula (see p. 50 in [47]) to have

$$\begin{aligned}
\mathcal{M}^{-1} &= \left((-2e^M + \mathbf{1}s^T) + s\mathbf{1}^T \right)^{-1} \\
&= -\frac{1}{2}e^{-M} - \frac{(e^{-M}\mathbf{1}s^T e^{-M})}{4 - 2s^T e^{-M}\mathbf{1}} \\
&\quad - \frac{\left(-\frac{1}{2}e^{-A} - \frac{(e^{-M}\mathbf{1}s^T e^{-M})}{4 - 2s^T e^{-M}\mathbf{1}} \right) s\mathbf{1}^T \left(-\frac{1}{2}e^{-M} - \frac{(e^{-M}\mathbf{1}s^T e^{-M})}{4 - 2s^T e^{-M}\mathbf{1}} \right)}{1 + \mathbf{1}^T \left(-\frac{1}{2}e^{-M} - \frac{(e^{-M}\mathbf{1}s^T e^{-M})}{4 - 2s^T e^{-M}\mathbf{1}} \right) s} \\
&= -\frac{1}{2}e^{-M} - \frac{ab}{4 - 2\varepsilon} - \frac{\left(-\frac{1}{2}b^T - \frac{ac}{4 - 2\varepsilon} \right) \left(-\frac{1}{2}a^T - \frac{db}{4 - 2\varepsilon} \right)}{1 + \left(-\frac{1}{2}\varepsilon - \frac{dc}{4 - 2\varepsilon} \right)},
\end{aligned} \tag{56}$$

from which we get

$$\mathcal{M}^{-1} = -\frac{1}{2}e^{-A} + \frac{caa^T - (\varepsilon - 2)b^T a^T - (\varepsilon - 2)ab + db^T b}{2(cd - (\varepsilon - 2)^2)}, \tag{57}$$

where $a = e^{-A}\mathbf{1}$, $b = s^T e^{-M}$, $c = s^T e^{-M}s$, $d = \mathbf{1}^T e^{-M}\mathbf{1}$, and $\varepsilon = s^T e^{-M}\mathbf{1}$. We still need to prove that the denominator is not zero: $cd - (\varepsilon - 2)^2 \neq 0$. It is easy to see that $c \geq \varepsilon$, with equality if and only if $s = \mathbf{1}$ which only happen if the graph is trivial, which is excluded here as the graphs are connected. Therefore,

$$-\varepsilon^2 + cd + 4\varepsilon - 4 > -\varepsilon^2 + (d + 4)\varepsilon - 4 > 0, \tag{58}$$

where the last inequality is obvious from the roots of the quadratic equation.

We now obtain $\mathbf{1}^T \mathcal{M}^{-1} \mathbf{1}$, as

$$\mathbf{1}^T \mathcal{M}^{-1} \mathbf{1} = -\frac{1}{2}d - \frac{d\varepsilon}{4 - 2\varepsilon} - \frac{\left(-\frac{1}{2}\varepsilon - \frac{dc}{4 - 2\varepsilon} \right) \left(-\frac{1}{2}d - \frac{d\varepsilon}{4 - 2\varepsilon} \right)}{1 + \left(-\frac{1}{2}\varepsilon - \frac{dc}{4 - 2\varepsilon} \right)} \tag{59}$$

$$= \frac{2d}{cd - (\varepsilon - 2)^2}. \tag{60}$$

Because $d = \mathbf{1}^T e^{-M}\mathbf{1}$ is the sum of all the entries of e^{-M} and $M \neq 0$ (because the graph is not trivial), we have that $d > 0$ and because we have proved before that $cd - (\varepsilon - 2)^2 > 0$, we have proved that \mathcal{M} is a nonsingular spherical EDM. \square

Remark 20 For properties of the circum-EDM \mathcal{M} when $M = A$, the reader is referred to [30, 36, 37]. For analysis of the circum-EDM \mathcal{M} when $M = L$, see [17, 82]. \square

7.2 Diffusive trajectories

In order to analyze the trajectories of the diffusive particles in a graph we need to convert the distances generated in the previous section into geodesics which can be traversed by these particles. That is, we need a geometrization of the graph. A graph is geometrized if we consider every edge $e = vw$ in E as a compact 1-dimensional manifold with boundary $\partial e = v \cup w$. We then assign to $e = vw$ the metric $\mathbb{L}_{vw}(M)$, such that, $\tilde{e}_{vw}(M) \cong [0, \mathcal{D}_{vw}(M)]$ if $e \in E$ or zero otherwise. In this way we transform the network into a space which is locally compact, complete and geodetic [15, 71].

Technically, what we need is to create the corresponding distance matrix $\mathcal{D}(M)$ and then multiply it in an entrywise way by A , creating a weighted adjacency matrix W in which every weight corresponds to the length of the corresponding edge. We now can obtain the weighted shortest paths (SP) connecting every pair of vertices. While the unweighted shortest paths correspond to the topological ones, those based on $\mathcal{D}(-L)$ correspond to the conservative diffusive SP, and the ones based on $\mathcal{D}(A)$ are the non-conservative diffusive SP, also known as communicability SP.

In Fig. 10 we illustrate the shortest topological (STP) and diffusive (conservative (SCP) and non-conservative (SNCP)) paths between a pair of vertices in a random rectangular graph. As expected, the STP crosses the vertices with the largest degree in the graph. However, the SNCP goes by a longer path to connect the same pair of origin-destination vertices, but in a way that avoids those highly connected vertices, not only in term of their degrees but in term of their general cliquishness. Somehow unexpected is the fact that the SCP is very similar to the STP, as it also crosses the most connected vertices in the graph.

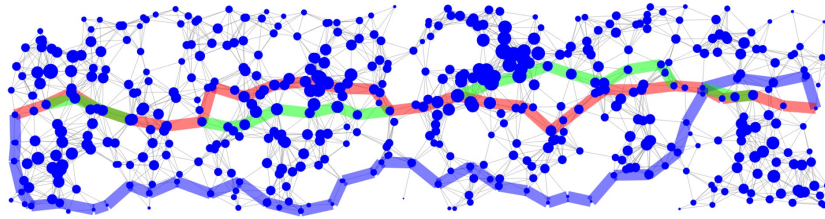


Fig. 10: Illustration of the diffusive paths between two vertices in a random rectangular graph. Blue: shortest non-conservative path (SNCP); Red: shortest conservative path (SCP); Green: shortest topological path (STP).

To understand the differences between the conservative and non-conservative diffusion trajectories let us first consider the non-conservative case. The non-conservative diffusion trajectory between two vertices corresponds to the path with the minimum sum of the corresponding distances $\mathcal{D}_{vw}(A)$ along the path. The distance between individual pairs of vertices can be written as

$$\begin{aligned} \mathcal{D}_{vw}(A) &= \left(1 + \frac{(A^2)_{vv}}{2!} + \frac{(A^3)_{vv}}{3!} + h.o\right) \\ &+ \left(1 + \frac{(A^2)_{ww}}{2!} + \frac{(A^3)_{ww}}{3!} + h.o\right) \\ &- 2 \left(A_{vw} + \frac{(A^2)_{vw}}{2!} + \frac{(A^3)_{vw}}{3!} + h.o\right), \end{aligned}$$

which can be written as

$$\begin{aligned} \mathcal{D}_{vw}(A) &= \left(1 + \frac{k_v}{2} + \frac{t_v}{3} + h.o\right) + \left(1 + \frac{k_w}{2} + \frac{t_w}{3} + h.o\right) \\ &- 2 \left(P_{vw}^1 + \frac{P_{vw}^2}{2!} + \frac{P_{vw}^3}{3!} + h.o\right), \end{aligned}$$

where k_i and t_i are the degree and the number of triangles of i , and P_{ij}^l is the number of paths of length l between i and j . Therefore, $\mathbb{L}_{vw}(A)$ avoids the vertices with the largest degree, largest number of triangles, etc., i.e., it avoids the vertices of largest cliquishness.

Let us now see what happens to $\mathcal{D}_{vw}(-L)$ along the path. We can write

$$\begin{aligned} \mathcal{D}_{vw}(-L) &= \left(1 - \frac{k_v}{2} - \frac{k_v^3}{6} - \frac{\sum_{(j,v) \in E} k_j}{6} + \frac{t_v}{6} + h.o\right) \\ &+ \left(1 - \frac{k_w}{2} - \frac{k_w^3}{6} - \frac{\sum_{(j,w) \in E} k_j}{6} + \frac{t_w}{6} + h.o\right) \\ &- 2 \left(-L_{vw} + \frac{(L^2)_{vw}}{2!} - \frac{(L^3)_{vw}}{3!} + h.o\right), \end{aligned}$$

indicating that $\mathbb{L}_{vw}(-L)$ does not necessarily avoid the vertices with high cliquishness as it has been the case of the example on Fig. 10.

7.3 Where to find non-conservative diffusion in graphs

We have seen in this chapter that the non-conservative diffusion has some advantages relative to conservative diffusion for finding a target on a networked environment. Namely, the steady state in the non-conservative process is reached much faster than in the conservative one by tracing trajectories that avoids the potentially most

connected vertices. Then, it is not surprising to find real-world systems in which non-conservative diffusion is present, some of which are described below.

The most intuitive of these examples is the one of traffic at rush hour that we have described in the Introduction. But, where does the “non-conservative” part come from? The number of cars departing from one intersection is not necessarily the same that arrives at the next one. The reason is that a few cars will end up their trajectory in the street leg between two intersections due to the existence of parking spaces in them. In a similar way some cars can emerge from these spaces, such that the number of cars can increase/decrease from one vertex to another.

A second illustrative example is the diffusive neurotransmission by means of chemical synapses in neuronal systems [78,91]. Nowadays it is well-established that chemical synapses do not only occur by the wiring intercellular communication in which two neurons interchange neurotransmitters [2]. Apart from this conservative process, neurons and brain regions also communicate by means of a volume transmission (VT), which uses the extracellular fluid filling channels of the extracellular space (ECS) and the cerebrospinal fluid filling ventricular space and sub-arachnoidal space [2, 13, 41, 85, 86, 94, 95]. That is, some amounts of the neurotransmitters are spilled over to the ECS in the perisynaptic region and from there it can be retaken by other neurons, or they can even be transported by blood and/or cerebrospinal fluid over long distances where they can also be retaken. From the point of view of the network of neuronal or brain regions, the process is clearly non-conservative, although at the organ-level it is of course a conservative process. Although not treated here, the process in which neurotransmitters, or other substances, are captured at longer distances from its origin by navigating across the reservoir allowing for long-range displacements resembles the mechanism of Levy flights in the setting of continuous diffusion, which is treated in this book. The current approach will be extended in the near future to consider these spatial nonlocalities as well as temporal ones.

A third example of networked non-conservative diffusion is the communication in social media [69, 80, 97] like Twitter or Facebook where a user can post a message which can be read by her followers, but also (if not constrained by the user) by non-followers, all of whom can propagate such information to others [88]. By constructing the network of followers, the propagation of information is non-conservative because part of the information leaves the network and some other information is subsequently received by the users from outside the network.

Other areas in which non-conservative diffusion on networks is present include, for instance, diffusive processes in ecology [12, 14, 83], diffusion of microplastics and other materials in the ocean [58] where the locations can be recorded by means of interconnected nodes, among others.

8 Conclusions

When referring to transmission principles in the brain, Tognoli and Scott-Kelso [89] stated that they “do not scale well upward from simple “channels” of synaptic

interactions to the larger and more complex web of evolved brains. Thus, it is without surprise that the brain betrays an essential communicational etiquette: its parts do not behave in a sequential—*one-talks-at-a-time*—manner”. This statement can be extended to most complex systems where the sender of information does not necessarily know the global topology of the network in which it is embedded.

The lack of a sequential *one-talks-at-a-time* communication is a characteristic feature of diffusive processes in which the sender of information spreads it across all potential routes to find its target(s). We have seen here that even a conservative diffusive way in which *one-talks-to-everybody* is not the most efficient way of reaching potential targets in networked environments. The discovery presented here by first time that the non-conservative diffusion is more efficient in communicating a source and a target in a network is somehow surprising. On the light of this discovery it is then clear why some new ways of social communication, such as online social networks, are so efficient in spreading information. They certainly use non-conservative diffusive ways of finding their targets. However, we should not forget that this process may be more costly energetically than a conservative one, particularly when diffusive particles need to be constantly created at the nodes of the network.

In the case of conservative diffusion we have previously extended the mathematical framework to consider quantum systems via the Schrödinger equation without potential on graphs [26]. In that case we considered a quantum walker on a graph which can hop not only to nearest neighbors but also to distant ones. The current framework of nonconservative diffusion with Lerman-Ghosh Laplacian can be mathematically extended to consider quantum nonconservative diffusion. The analysis of this theoretical scenario opens new avenues for the study of quantum processes on graphs. Other plausible frameworks for extending the current approaches are the consideration of biased Laplacians [27, 42, 75] or its combination with centrality-based stochastic resetting of random walks [96].

The current work also opens new avenues that should be explored to better understand the ways in which source-to-target communication occurs in complex systems. For instance, anomalous diffusion on graphs described by means of the d -path Laplacians [24, 28, 34, 35] and its combination with fractional temporal derivatives [19], are all conservative processes. The extension of d -path Laplacians to d -path Lerman-Ghosh Laplacians seems to be a necessary extension of the current work. This will allow us to investigate, for instance, if the non-conservative anomalous diffusion is more efficient than its conservative analogous in finding a target on a graph. Similarly, the Lerman-Ghosh Laplacians can be used in degree-biased advection-diffusion models on undirected graphs/networks [75] to simulate realistic scenarios in complex systems. Another avenue is to investigate non-conservative diffusion in metaplexes [32], where not only the particles diffuse across a discrete space, but also in a continuous one existing inside the nodes. All in all, we hope this Chapter helps the readers in their particular “Target Problems” for understanding complex systems. The author thanks Project OLGRA (PID2019-107603GB-I00) funded by Spanish Ministry of Science and Innovation and the Maria de Maeztu project CEX2021-001164-M funded by the MCIN/AEI/10.13039/501100011033.

References

1. Abadias, L., Estrada-Rodríguez, G., and Estrada, E. (2020). Fractional-order susceptible-infected model: definition and applications to the study of covid-19 main protease. *Fractional Calculus and Applied Analysis*, 23(3):635–655.
2. Agnati, L. F., Guidolin, D., Guescini, M., Genedani, S., and Fuxe, K. (2010). Understanding wiring and volume transmission. *Brain research reviews*, 64(1):137–159.
3. Akbarzadeh, M. and Estrada, E. (2018). Communicability geometry captures traffic flows in cities. *Nature human behaviour*, 2(9):645–652.
4. Alfakih, A. (2006). A remark on the faces of the cone of euclidean distance matrices. *Linear algebra and its applications*, 414(1):266–270.
5. Arrigo, F. and Durastante, F. (2021). Mittag–leffler functions and their applications in network science. *SIAM Journal on Matrix Analysis and Applications*, 42(4):1581–1601.
6. Bacaër, N. and Bacaër, N. (2011). Verhulst and the logistic equation (1838). *A short history of mathematical population dynamics*, pages 35–39.
7. Bellman, R. (1958). On a routing problem. *Quarterly of applied mathematics*, 16(1):87–90.
8. Berge, C. (2001). *The theory of graphs*. Courier Corporation.
9. Bonacich, P. (1971). Factoring and weighing approaches to clique identification. *Journal of Mathematical Sociology*, 92:1170–1182.
10. Bonacich, P. (1987). Power and centrality: A family of measures. *American journal of sociology*, 92(5):1170–1182.
11. Bonacich, P. (2007). Some unique properties of eigenvector centrality. *Social networks*, 29(4):555–564.
12. Borrett, S. R. and Patten, B. C. (2003). Structure of pathways in ecological networks: Relationships between length and number. *Ecological Modelling*, 170(2-3):173–184.
13. Borroto-Escuela, D. O., Perez De La Mora, M., Manger, P., Narváez, M., Beggiano, S., Crespo-Ramírez, M., Navarro, G., Wydra, K., Díaz-Cabiale, Z., Rivera, A., et al. (2018). Brain dopamine transmission in health and parkinson’s disease: modulation of synaptic transmission and plasticity through volume transmission and dopamine heteroreceptors. *Frontiers in synaptic neuroscience*, 10:20.
14. Brännström, Å. and Sumpter, D. J. (2005). Coupled map lattice approximations for spatially explicit individual-based models of ecology. *Bulletin of mathematical biology*, 67(4):663–682.
15. Bridson, M. R. and Haefliger, A. (2013). *Metric spaces of non-positive curvature*, volume 319. Springer Science & Business Media.
16. Brogueira, P. and de Deus, J. D. (2010). Evolution equation for soft physics at high energy. *Journal of Physics G: Nuclear and Particle Physics*, 37(7):075006.
17. Coifman, R. R. and Lafon, S. (2006). Diffusion maps. *Applied and computational harmonic analysis*, 21(1):5–30.
18. Crank, J. (1979). *The mathematics of diffusion*. Oxford university press.
19. Diaz-Diaz, F. and Estrada, E. (2022). Time and space generalized diffusion equation on graph/networks. *Chaos, Solitons & Fractals*, 156:111791.
20. Dijkstra, E. W. (2022). A note on two problems in connexion with graphs. In *Edsger Wybe Dijkstra: His Life, Work, and Legacy*, pages 287–290.
21. El-Hachem, M., McCue, S. W., Jin, W., Du, Y., and Simpson, M. J. (2019). Revisiting the fisher–kolmogorov–petrovsky–piskunov equation to interpret the spreading–extinction dichotomy. *Proceedings of the Royal Society A*, 475(2229):20190378.
22. Erdős, P. and Rényi, A. (1959). On random graphs i. *Publ. math. debrecen*, 6(290-297):18.
23. Estrada, E. (2012a). The communicability distance in graphs. *Linear Algebra and its Applications*, 436(11):4317–4328.
24. Estrada, E. (2012b). Path laplacian matrices: introduction and application to the analysis of consensus in networks. *Linear algebra and its applications*, 436(9):3373–3391.
25. Estrada, E. (2012c). *The structure of complex networks: theory and applications*. Oxford University Press, USA.
26. Estrada, E. (2020a). d-path laplacians and quantum transport on graphs. *Mathematics*, 8(4):527.

27. Estrada, E. (2020b). 'hubs-repelling' laplacian and related diffusion on graphs/networks. *Linear Algebra and Its Applications*, 596:256–280.
28. Estrada, E. (2021). Path laplacians versus fractional laplacians as nonlocal operators on networks. *New Journal of Physics*, 23(7):073049.
29. Estrada, E. (2022). The many facets of the estrada indices of graphs and networks. *SeMA Journal*, 79(1):57–125.
30. Estrada, E. (2023a). Every nonsingular spherical euclidean distance matrix is a resistance distance matrix. *Linear Algebra and its Applications*, 656:198–209.
31. Estrada, E. (2023b). What is a complex system, after all? *Foundations of Science*, pages 1–28.
32. Estrada, E., Estrada-Rodriguez, G., and Gimperlein, H. (2020). Metaplex networks: Influence of the exo-endo structure of complex systems on diffusion. *SIAM Review*, 62(3):617–645.
33. Estrada, E., Gómez-Gardeñes, J., and Lacasa, L. (2023). Network bypasses sustain complexity. *Proceedings of the National Academy of Sciences*, 120(31):e2305001120.
34. Estrada, E., Hameed, E., Hatano, N., and Langer, M. (2017). Path laplacian operators and superdiffusive processes on graphs. i. one-dimensional case. *Linear Algebra and its Applications*, 523:307–334.
35. Estrada, E., Hameed, E., Langer, M., and Puchalska, A. (2018). Path laplacian operators and superdiffusive processes on graphs. ii. two-dimensional lattice. *Linear Algebra and its Applications*, 555:373–397.
36. Estrada, E. and Hatano, N. (2016). Communicability angle and the spatial efficiency of networks. *SIAM Review*, 58(4):692–715.
37. Estrada, E., Sanchez-Lirola, M., and De La Peña, J. A. (2014). Hyperspherical embedding of graphs and networks in communicability spaces. *Discrete Applied Mathematics*, 176:53–77.
38. Fisher, R. A. (1937). The wave of advance of advantageous genes. *Annals of eugenics*, 7(4):355–369.
39. Floyd, R. W. (1962). Algorithm 97: shortest path. *Communications of the ACM*, 5(6):345.
40. Ford, L. R. (1956). *Network flow theory*. Rand Corporation Santa Monica, CA.
41. Fuxe, K., Borroto-Escuela, D. O., Tarakanov, A., Fernandez, W. R., Manger, P., Rivera, A., van Craenenbroeck, K., Skieterska, K., Diaz-Cabiale, Z., Filip, M., et al. (2013). Understanding the balance and integration of volume and synaptic transmission. relevance for psychiatry. *Neurology, Psychiatry and Brain Research*, 19(4):141–158.
42. Gambuzza, L. V., Frasca, M., and Estrada, E. (2020). Hubs-attracting laplacian and related synchronization on networks. *SIAM Journal on Applied Dynamical Systems*, 19(2):1057–1079.
43. Garrappa, R. and Popolizio, M. (2018). Computing the matrix mittag-leffler function with applications to fractional calculus. *Journal of Scientific Computing*, 77(1):129–153.
44. Ghosh, R. and Lerman, K. (2011). Parameterized centrality metric for network analysis. *Physical Review E*, 83(6):066118.
45. Ghosh, R., Lerman, K., Surachawala, T., Voevodski, K., and Teng, S.-H. (2011). Non-conservative diffusion and its application to social network analysis. *arXiv preprint arXiv:1102.4639*.
46. Gillespie, D. T. and Seitaridou, E. (2013). *Simple Brownian diffusion: an introduction to the standard theoretical models*. Oxford University Press, USA.
47. Golub, G. H. and Van Loan, C. F. (1996). *Matrix computations*. Johns Hopkins University Press, 3rd edition.
48. Golden, B. (1976). Shortest-path algorithms: A comparison. *Operations Research*, 24(6):1164–1168.
49. Golledge, R. G. and Gärling, T. (2004). Cognitive maps and urban travel. In *Handbook of transport geography and spatial systems*, pages 501–512. Emerald Group Publishing Limited.
50. Goñi, J., Avena-Koenigsberger, A., Velez de Mendizabal, N., van den Heuvel, M. P., Betzel, R. F., and Sporns, O. (2013). Exploring the morphospace of communication efficiency in complex networks. *PLoS One*, 8(3):e58070.
51. Gower, J. C. (1985). Properties of euclidean and non-euclidean distance matrices. *Linear algebra and its applications*, 67:81–97.
52. Grebenkov, D. S. and Tupikina, L. (2018). Heterogeneous continuous-time random walks. *Physical Review E*, 97(1):012148.

53. Grigor'yan, A. (2018). *Introduction to analysis on graphs*, volume 71. American Mathematical Soc.
54. Grone, R. and Merris, R. (1994). The laplacian spectrum of a graph ii. *SIAM Journal on discrete mathematics*, 7(2):221–229.
55. Grone, R., Merris, R., and Sunder, V. (1990). The laplacian spectrum of a graph. *SIAM Journal on matrix analysis and applications*, 11(2):218–238.
56. Hernando, A. and Plastino, A. (2013). Scale-invariance underlying the logistic equation and its social applications. *Physics Letters A*, 377(3-4):176–180.
57. Higham, N. J. (2008). *Functions of matrices: theory and computation*. SIAM.
58. Isobe, A., Iwasaki, S., Uchida, K., and Tokai, T. (2019). Abundance of non-conservative microplastics in the upper ocean from 1957 to 2066. *Nature communications*, 10(1):417.
59. Jaklič, G. and Modic, J. (2013). On euclidean distance matrices of graphs. *The Electronic Journal of Linear Algebra*, 26:574–589.
60. Keil, M. S. (2008). Local to global normalization dynamic by nonlinear local interactions. *Physica D: Nonlinear Phenomena*, 237(6):732–744.
61. Kim, S.-S., Chung, M., and Kim, Y.-K. (2020). Urban traffic prediction using congestion diffusion model. In *2020 IEEE International Conference on Consumer Electronics-Asia (ICCE-Asia)*, pages 1–4. IEEE.
62. Kolmogorov, A. N., Petrovsky, I. G., and Piskunov, N. S. (1937). A study of the equation of diffusion with increase in the quantity of matter, and its application to a biological problem. *Moscow University Bulletin of Mathematics*, 1:1–25.
63. Kooi, B., Boer, M., and Kooijman, S. (1998). On the use of the logistic equation in models of food chains. *Bulletin of mathematical biology*, 60(2):231–246.
64. Kwapień, J. and Drożdż, S. (2012). Physical approach to complex systems. *Physics Reports*, 515(3-4):115–226.
65. Lee, C.-H., Tenneti, S., and Eun, D. Y. (2019). Transient dynamics of epidemic spreading and its mitigation on large networks. In *Proceedings of the twentieth ACM international symposium on mobile ad hoc networking and computing*, pages 191–200.
66. Lenzi, E., Mendes, R., and Tsallis, C. (2003). Crossover in diffusion equation: Anomalous and normal behaviors. *Physical Review E*, 67(3):031104.
67. Li, C.-K., Milligan, T., and Trosset, M. (2010). Euclidean and circum-euclidean distance matrices: Characterizations and linear preservers. *The Electronic Journal of Linear Algebra*, 20:739–752.
68. Liu, J., Li, M., Pan, Y., Lan, W., Zheng, R., Wu, F.-X., Wang, J., et al. (2017). Complex brain network analysis and its applications to brain disorders: a survey. *Complexity*, 2017.
69. Liu, L., Tang, J., Han, J., and Yang, S. (2012). Learning influence from heterogeneous social networks. *Data mining and knowledge discovery*, 25:511–544.
70. Măntoiu, M., Richard, S., and de Aldecoa, R. T. (2007). Spectral analysis for adjacency operators on graphs. In *Annales Henri Poincaré*, volume 8, pages 1401–1423. Springer.
71. Markvorsen, S. (2008). Minimal webs in riemannian manifolds. *Geometriae Dedicata*, 133:7–34.
72. Masuda, N., Porter, M. A., and Lambiotte, R. (2017). Random walks and diffusion on networks. *Physics reports*, 716:1–58.
73. Merris, R. (1995). A survey of graph laplacians. *Linear and Multilinear Algebra*, 39(1-2):19–31.
74. Mesbahi, M. and Egerstedt, M. (2010). *Graph theoretic methods in multiagent networks*. Princeton University Press.
75. Miranda, M. and Estrada, E. (2022). Degree-biased advection–diffusion on undirected graphs/networks. *Mathematical Modelling of Natural Phenomena*, 17:30.
76. Mohar, B., Alavi, Y., Chartrand, G., and Oellermann, O. (1991). The laplacian spectrum of graphs. *Graph theory, combinatorics, and applications*, 2(871-898):12.
77. Moore, E. F. (1959). The shortest path through a maze. In *Proceedings of the International Symposium on the Theory of Switching*, pages 285–292. Harvard University Press.
78. Nicholson, C. (2001). Diffusion and related transport mechanisms in brain tissue. *Reports on progress in Physics*, 64(7):815.

79. Olfati-Saber, R., Fax, J. A., and Murray, R. M. (2007). Consensus and cooperation in networked multi-agent systems. *Proceedings of the IEEE*, 95(1):215–233.
80. Overbey, L. A., Greco, B., Paribello, C., and Jackson, T. (2013). Structure and prominence in twitter networks centered on contentious politics. *Social Network Analysis and Mining*, 3:1351–1378.
81. Schoenberg, I. J. (1938). Metric spaces and positive definite functions. *Transactions of the American Mathematical Society*, 44(3):522–536.
82. Scott, C. and Mjolsness, E. (2021). Graph diffusion distance: Properties and efficient computation. *Plos one*, 16(4):e0249624.
83. Scott, D. (1965). The determination and use of thermodynamic data in ecology. *Ecology*, 46(5):673–680.
84. Sokolov, I. M. (2012). Models of anomalous diffusion in crowded environments. *Soft Matter*, 8(35):9043–9052.
85. Sykova, E. (2004). Extrasynaptic volume transmission and diffusion parameters of the extracellular space. *Neuroscience*, 129(4):861–876.
86. Taber, K. H. and Hurley, R. A. (2014). Volume transmission in the brain: beyond the synapse. *The Journal of neuropsychiatry and clinical neurosciences*, 26(1):iv–4.
87. Tarazaga, P., Hayden, T., and Wells, J. (1996). Circum-euclidean distance matrices and faces. *Linear Algebra and its Applications*, 232:77–96.
88. Taxidou, I. and Fischer, P. M. (2014). Online analysis of information diffusion in twitter. In *Proceedings of the 23rd international conference on world wide web*, pages 1313–1318.
89. Tognoli, E. and Kelso, J. S. (2014). Enlarging the scope: grasping brain complexity. *Frontiers in systems neuroscience*, 8:122.
90. Tomasi, D., Wang, G.-J., and Volkow, N. D. (2013). Energetic cost of brain functional connectivity. *Proceedings of the National Academy of Sciences*, 110(33):13642–13647.
91. Tønnesen, J., Hrabětová, S., and Soria, F. N. (2023). Local diffusion in the extracellular space of the brain. *Neurobiology of Disease*, 177:105981.
92. Wang, X. Z. (2018). The comparison of three algorithms in shortest path issue. In *Journal of Physics: Conference Series*, volume 1087, page 022011. IOP Publishing.
93. Warshall, S. (1962). A theorem on boolean matrices. *Journal of the ACM*, 9(1):11–12.
94. Wiencke, K., Horstmann, A., Mathar, D., Villringer, A., and Neumann, J. (2020). Dopamine release, diffusion and uptake: A computational model for synaptic and volume transmission. *PLOS Computational Biology*, 16(11):e1008410.
95. Xiong, H., Lacin, E., Ouyang, H., Naik, A., Xu, X., Xie, C., Youn, J., Wilson, B. A., Kumar, K., Kern, T., et al. (2022). Probing neuropeptide volume transmission in vivo by simultaneous near-infrared light-triggered release and optical sensing. *Angewandte Chemie*, 134(34):e202206122.
96. Zelenkovski, K., Sandev, T., Metzler, R., Kocarev, L., and Basnarkov, L. (2023). Random walks on networks with centrality-based stochastic resetting. *Entropy*, 25(2):293.
97. Zeng, A. and Yeung, C. H. (2016). Predicting the future trend of popularity by network diffusion. *Chaos: An Interdisciplinary Journal of Nonlinear Science*, 26(6).
98. Zhang, C., Bai, H., Wang, S., and Xie, C. (2018). Review of urban traffic congestion formation and diffusion mechanism. In *CICTP 2015*, pages 2376–2385.
99. Zhang, H., Zhao, X., Yu, X., Liu, L., and Ma, S. (2016). Complex network characteristics and evolution research of software architecture. In *2016 IEEE Advanced Information Management, Communicates, Electronic and Automation Control Conference (IMCEC)*, pages 1785–1788. IEEE.
100. Zhao, L. and Zhao, J. (2017). Comparison study of three shortest path algorithm. In *2017 International Conference on Computer Technology, Electronics and Communication (ICCTEC)*, pages 748–751. IEEE.